



3-D position sensitive CdZnTe gamma-ray spectrometers

Z. He^{a,*}, W. Li^a, G.F. Knoll^a, D.K. Wehe^a, J. Berry^a, C.M. Stahle^b

^a *Department of Nuclear Engineering and Radiological Sciences, University of Michigan, Ann Arbor, MI 48109, USA*

^b *Orbital Sciences Corp./NASA Goddard Space Flight Center, Code 553, Greenbelt, MD 20771, USA*

Abstract

Two 3-D position-sensitive room temperature semiconductor γ -ray spectrometers have been built using 1 cm^3 cubic CdZnTe crystals. The lateral coordinates of γ -ray interaction are obtained from the location of the $11(x) \times 11(y)$ pixellated anodes and the depth (z) is obtained from the ratio of the signals coming from the cathode and the anode. Energy spectra from 662 keV incident γ -rays have been collected from each of the $11(x) \times 11(y) \times 20(z)$ voxels in both of the CdZnTe devices. After corrections for electron trapping, the difference of weighting potentials in 3-D, and for the gain variation of the readout circuitry, energy resolutions of 1.70% (11.3 keV) FWHM and 1.84% (12.2 keV) FWHM were obtained at 662 keV γ -ray energy on the first and second detectors, respectively, from the whole bulk for single-pixel events. Possible improvements in the detector performance are discussed. © 1999 Elsevier Science B.V. All rights reserved.

1. Introduction

By combining 2-D position sensing using a pixelated anode array [1] yielding good energy resolution from the small pixel effect [2], and the depth sensing technique [3,4] for electron trapping corrections, the first two 3-D position sensitive CdZnTe γ -ray spectrometers have been fabricated.

An 11×11 pixellated anode array was fabricated on one $10 \times 10\text{ mm}$ surface of each 1 cm^3 cube CdZnTe crystal at NASA Goddard Space Flight Center. The details for the fabrication process to achieve good metal electrodes for wire bonding and high surface resistivity was published previously

[5]. The (x, y) coordinates (in the plane parallel to the anode surface) of γ -ray interactions are obtained from the location of the pixel anode where electrons are collected. Instead of using an array of simple square pixel anodes [1], each square anode is surrounded by a common non-collecting grid which is biased at a potential lower than that of pixel anodes [6]. As shown in Fig. 1, each pixel has a dimension of $0.7 \times 0.7\text{ mm}$, with a collecting anode of $0.2 \times 0.2\text{ mm}$ at the center surrounded by a common non-collecting grid with a width of 0.1 mm. Since the non-collecting grid is biased at lower potential relative to that of the collecting anodes, electrons are guided towards the collecting pixel anodes. More importantly, the dimension of the pixel anode that is smaller than the pixel dimension enhances the small pixel effect and minimizes any induced signal from the movement of holes.

*Corresponding author. E-mail: hezhong@engin.umich.edu.

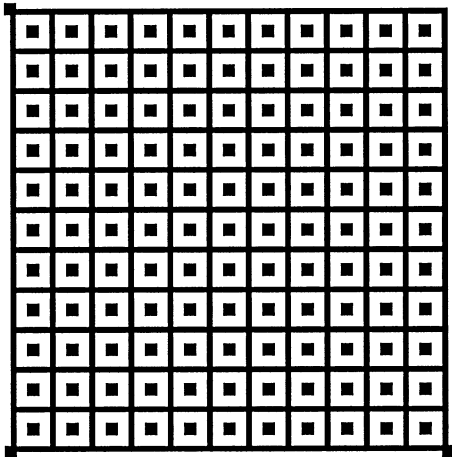


Fig. 1. Top view of pixellated anode.

The 11×11 anode array covers an area of 7.8×7.8 mm on the 10×10 mm CdZnTe anode surface. The gaps between the boundary of the non-collecting grid and the edges of the crystal facilitated the fabrication, but resulted in an effective volume of peripheral pixels, especially the four corner pixels, that is larger than the volume of each of 9×9 central pixels. A picture of the CdZnTe detector wirebonded to the fanout board which is then wirebonded to the readout ASIC (VA1 chip) is shown in Fig. 2.

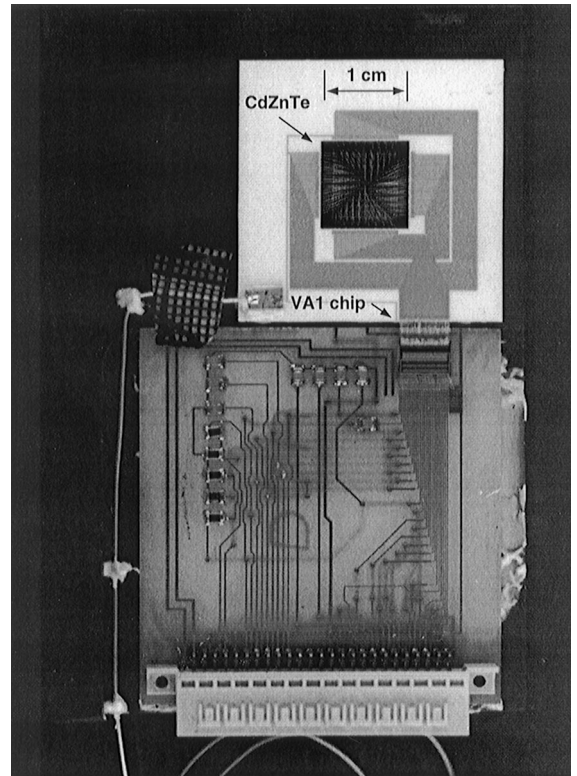


Fig. 2. A picture of the detector system.

2. Depth sensing

The γ -ray interaction depth between the cathode and the anode is obtained from the ratio of the cathode and the anode signals [3,4]. This technique provides the depth (z) of the γ -ray interaction for single-site events, and the centroid depth for multiple-site interactions, such as Compton scattering events.

In order to identify individual γ -ray interaction depths for multiple-site events, the signal from the non-collecting grid is read out using an A250 [7] charge sensitive preamplifier. When electrons generated by an energy deposition are deflected towards the collecting pixel anode near the anode surface, a negative pulse is induced on the non-collecting grid as shown in Fig. 3. A differential

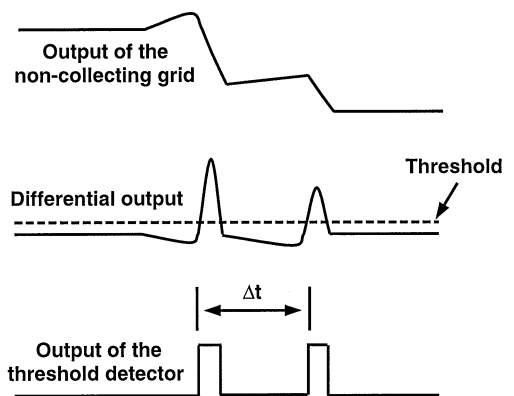


Fig. 3. Illustration of depth sensing for multiple-site events.

circuit provides a positive pulse corresponding to the negative drop of the non-collecting grid signal. A threshold circuit uses the differential output to produce a logic pulse when the differential signal is

above the set threshold. The threshold circuit triggers the data acquisition system, and provides start and stop signals to a time-to-amplitude converter (TAC) so that the interval of drifting times of electron clouds can be measured. By combining the centroid depth, pulse amplitudes from each pixel anode and the depth interval between energy depositions, the depth of each individual energy deposition can be obtained.

Although the differential circuit can identify multiple γ -ray interaction depths, the TAC limits the number of interactions to two. Therefore, the current system provides γ -ray interaction depths for only single and two-site events. Events having more energy depositions than two can be identified by the number of anode pixels with recorded signals, but only the centroid interaction depth can be obtained. The threshold on the grid signal is relatively high at about 100 keV in the present measurements.

3. Data acquisition system

The data acquisition system is schematically shown in Fig. 4. Signals induced on the 11×11 pixel anodes are read out by VA1 integrated circuitry [8] which has 128 channels of independent preamplifiers, shaping amplifiers and sample/holds. The cathode signal is processed by an A250 preamplifier followed by an EG&G Ortec 572 shaping amplifier with a shaping time constant of $0.5 \mu\text{s}$. Since the sample/hold signal required by the VA1 circuitry holds the pulse amplitudes of all 128 channels simultaneously, the peak amplitudes of Comp-

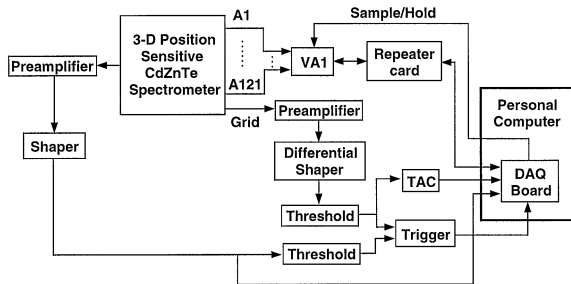


Fig. 4. The schematic diagram of the data acquisition system.

ton scattering events will not be obtained correctly by the fixed sample/hold time due to different pulse peaking times. Because of the high threshold needed due to the poor signal-to-noise ratio of the grid signal, the trigger is instead taken from the cathode signal for low energy γ -ray events. By using the combination of the grid and the cathode triggers, γ -rays within the whole energy range can be collected. For simplicity, the grid trigger was used for higher energy γ -ray sources, such as ^{137}Cs , and the trigger from the cathode signal was used for low energy γ -rays, such as ^{241}Am , in our measurements.

4. γ -Ray spectroscopy

Both 1 cm^3 cubic 3-D position sensitive CdZnTe spectrometers have been tested using a $10 \mu\text{Ci}$ ^{137}Cs source located about 5 cm from the cathode surface. The biases between the cathode and the anode were 2000 and 1400 V for the two devices, and the biases between the pixel anodes and the non-collecting grid were 50 and 30 V, respectively. The lower voltages used on the second device were dictated by higher leakage currents which saturated the preamplifiers on the VA1 chip. Energy spectra were measured sorted by the number of pixels producing signals per incident gamma.

Fig. 5 shows the energy spectra obtained from pixel anode #6 of the first detector as a function of

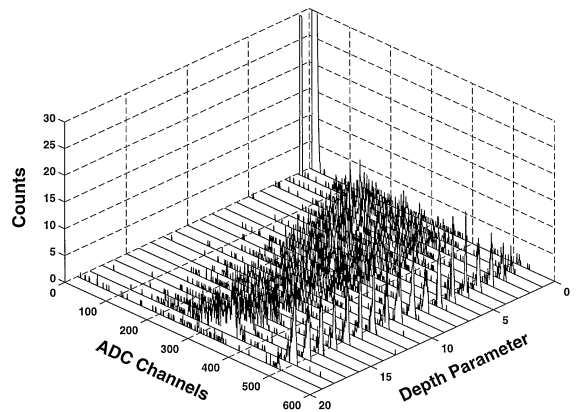


Fig. 5. Energy spectra of ^{137}Cs obtained from pixel #6 of the first detector at different depths.

20 γ -ray interaction depths ranging from near the anode surface to the cathode surface. Single-pixel events, including multiple interactions depositing energy within the column underneath one anode pixel, were selected for the spectra. The energy threshold for rejection of multiple-pixel events was ~ 10 keV. Since a depth resolution of less than 0.5 mm can be achieved at 662 keV γ -ray energy [4], spectra were binned into 20 depths. Thus each of the 2420 resolved voxels corresponds to a volume of about $0.7(x) \times 0.7(y) \times 0.5(z)$ mm in the detector.

The centroids of 662 keV photopeak amplitudes from each voxel were measured. Electron trapping can be observed from the significant decrease in pulse amplitude with increasing electron drift distance as shown in Fig. 6. The sharp drop in photopeak amplitude near the anode surface (depth parameter < 3) is caused by the non-linear weighting potential in the vicinity of the anode surface. The correction for electron trapping, the effect of the weighting potential, and the electronic gain variation is performed by applying a multiplicative constant to the pulse amplitude depending on the voxel and the energy deposition (if necessary), so that the photopeak centroids of all voxels are aligned at each γ -ray energy.

After these corrections, the energy spectrum of 662 keV γ -rays was obtained from the whole bulk

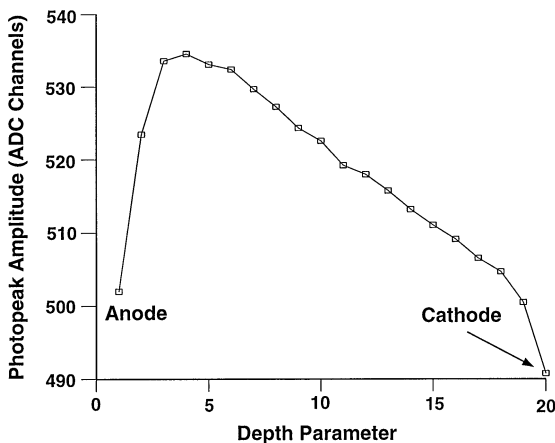


Fig. 6. The centroids of ^{137}Cs photopeak amplitudes as a function of the depth parameter (1–20) from pixel #6 of the first detector.

for single-pixel events. The result, as shown in Fig. 7, yielded energy resolutions of 1.70% (11.3 keV) FWHM and 1.84% (12.2 keV) FWHM from the two devices.

Since there is a gap of ~ 1 mm left between the boundary of the non-collecting grid and the edges of the 1 cm square CdZnTe surface, the effective volume and the charge collection of peripheral pixels are different from that of central pixels. In order to isolate the detector performance from this edge effect, the energy spectra of 662 keV γ -rays were collected from just the central 9×9 pixels. Energy resolutions of 1.51% (10.0 keV) FWHM (see Fig. 8) and 1.74% (11.5 keV) FWHM were obtained from the two devices respectively.

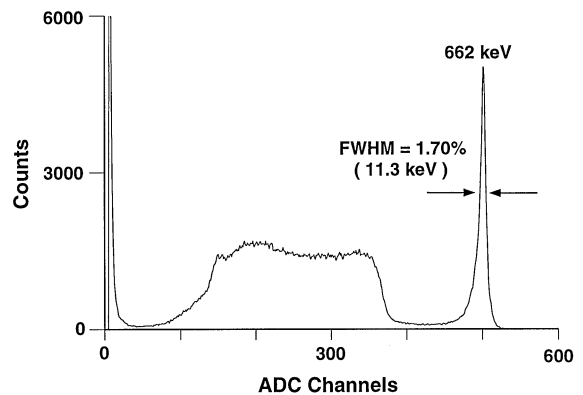


Fig. 7. Energy spectrum of ^{137}Cs obtained from the whole bulk of the first detector for single-pixel events.

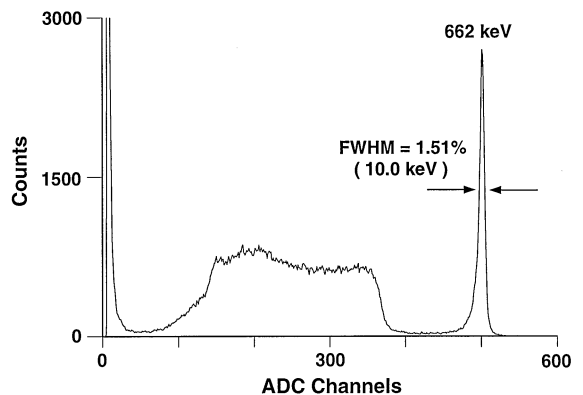


Fig. 8. Energy spectrum of ^{137}Cs obtained from the central 9×9 pixels of the first detector for single-pixel events.

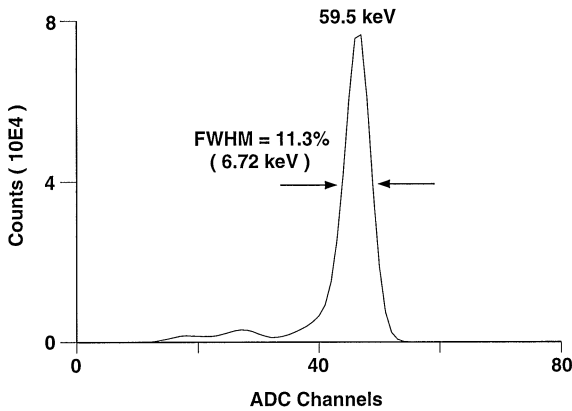


Fig. 9. Energy spectrum of ^{241}Am obtained from the whole bulk of the first detector for single-pixel events.

The first detector was also tested at 60 keV using a ^{241}Am source located ~ 5 cm from the cathode surface. After the correction for electronic gain variation, an energy resolution of 11.3% (6.7 keV) FWHM was obtained (see Fig. 9).

5. Discussions

There are several factors which limited the detector performance. First, the VA1 chip was designed for very low leakage current at its inputs. The feedback FETs on the VA1 preamplifiers must be operated in an ad hoc status to prevent preamplifier saturation by the leakage current of even a few nA from each pixel anode. The electronic noise thus increased from ~ 3 keV to 6–7 keV FWHM. The electronic noise should reduce to ~ 3 keV FWHM if AC coupling or equivalent circuitry between the pixellated anodes and the VA1 chip replaces the DC coupling currently used. Second, the sample/hold signal required by the VA1 chip holds the pulse amplitude of all 128 channels simultaneously. For Compton scattering events, the peak amplitudes can not be correctly sampled due to the variable electron drifting times. This leads to significant degradation in energy resolution for multiple-pixel events. The energy resolution of ^{137}Cs for two pixel events was 3.7% (24.5 keV) FWHM on the first detector, which is significantly worse than that predicted from the

results of single-pixel events. Third, while γ -ray Monte Carlo simulations using GEANT3 [9] indicate that $\sim 50\%$ of 662 keV γ -ray interactions should be registered as single-pixel events when electron cloud size is not considered, only 25% and 15% of 662 keV γ -ray events were recorded as single-pixel events on the two detectors. This discrepancy indicates that the actual size of the electron clouds increases the fraction of multiple-pixel events. Since the energy resolution degrades when the number of pixels which record signals increases, the optimum pixel dimension should be large enough to minimize charge sharing between anode pixels, yet small enough to correct for the non-uniformity of the detector material and produce the small pixel effect.

Both 1 cm^3 cubic CdZnTe detectors were fabricated using discrimination grade crystals [10]. Significant material defects were observed within the bulk of the second device. These defects may account for the higher leakage current and the low fraction of single-pixel events compared with the first device (which showed a much uniform γ -ray response within the detector volume). Thus we feel that the measured energy resolutions do not represent the limitations of future 3-D position sensitive CdZnTe spectrometers, especially for multiple-pixel events. Our initial investigation has been focused on the single and two-site interaction events, which account for $\sim 60\%$ of 662 keV γ -ray interactions collected.

Acknowledgements

This work was supported under DOE Grant DOE-FG08-94NV11630. We thank N.A. Blum, J.S. Lehtonen and R.P. Aylor of Johns Hopkins University Applied Physics Lab. for their work on the wire bonds and detector assembly, and F. Schoper of Max-Planck-Institute for help in our data acquisition system.

References

- [1] F.P. Doty et al., Nucl. Instr. and Meth. A 353 (1994) 356.
- [2] H.H. Barrett et al., Phys. Rev. Lett. 75 (1) (1995) 156.

- [3] Z. He et al., Nucl. Instr. and Meth. A 380 (1996) 228.
- [4] Z. He et al., Nucl. Instr. and Meth. A 388 (1997) 180.
- [5] C.M. Stahle et al., Proc SPIE 3115 (1997) 90.
- [6] Z. He, Nucl. Instr. and Meth. A 365 (1995) 572.
- [7] Amptek Inc., 6 De Angelo Drive, Bedford, MA 01730, USA.
- [8] IDE AS, Veritasveien 9, N-1322 Hovik, Norway.
- [9] GEANT3, CERN, Geneva, Switzerland.
- [10] eV Products, 375 Saxonburg Boulevard, Saxonburg, PA 16056, USA.